Skvarla, J.; Raya, R.K.; Uchman, M.; Zednik, J.; Prochazka, K.;
Haramus, V.M.; Meristoudi, A.; Pispas, S.; Stepanek, M..:

Thermoresponsive behavior of poly(Nue-isopropylacrylamide)s with dodecyl and carboxyl terminal groups in aqueous solution: pH-dependent cloud point temperature

In: Colloid and Polymer Science (2017) Springer

DOI: 10.1007/s00396-017-4067-z

Thermoresponsive behavior of poly(N-Isopropylacrylamide)s with dodecyl and carboxyl terminal groups in aqueous solution: pH-dependent cloud point temperature

Juraj Škvarla[1], Rahul K. Raya[1], Mariusz Uchman[1], Jiří Zedník[1], Karel Procházka[1], Vasil M. Garamus[2], Anastasia Meristoudi[3], Stergios Pispas[3] and Miroslav Štěpánek[1,*]

[1]*Department of Physical and Macromolecular Chemistry, Faculty of Science Charles University in Prague, Hlavova 2030, 12840 Prague 2, Czech Republic*
[2]*Helmholtz-Zentrum Geesthacht, Centre for Materials and Coastal Research, D-21502 Geesthacht, Germany*
[3]*Theoretical & Physical Chemistry Institute, National Hellenic Research Foundation, 48 Vassileos Constantinou Ave., 11635 Athens, Greece*

*e–mail: stepanek@natur.cuni.cz

Abstract

It was recently reported that poly(*N*-isopropyl acrylamide) (PNIPAm) polymers synthesized by RAFT polymerization using S-1-dodecyl-S$^{'}$-(α,α$^{'}$-dimethyl-α$^{''}$-acetic acid)trithiocarbonate as a chain transfer agent form micelles in aqueous solutions with the core of hydrophobic terminal dodecyl groups and the corona of PNIPAm chains with carboxylic groups at the periphery, the ionization of which prevents PNIPAm from phase separation above its lower critical solution temperature in water (Langmuir 30:7986–7992). In this paper, we study the pH- and ionic strength-dependence of the aggregation behavior of two HOOC-PNIPAm-C12 polymers, differing in the degree of polymerization, in aqueous solutions. We show that changing pH of the solution allows for shifting the cloud point temperature (CPT) of the polymers up to several tens of K. The aggregation of the PNIPAms above the CPT can be efficiently accelerated by screening electrostatic repulsion between PNIPAm micelles by changing ionic strength of the solution.

Keywords thermoresponsive polymers, aggregation, self-assembly, small-angle scattering, micelles

Introduction

Poly(N-isopropyl acrylamide) (PNIPAm) is one of the most frequently studied thermosensitive polymers, both as a subject of fundamental research and with respect to its potential applications in thermoresponsive systems for controlled drug release, due to its biocompatibility and due to its application-suitable lower critical solution temperature (LCST) in water at 32°C [1–3]. Above the LCST, microphase separation rather than macroscopic phase separation occurs resulting in the formation of nanoaggregates of the polymer [4,5]. Therefore the phase transition temperature at a given PNIPAm concentration is usually detected by the increase in the solution turbidity as the cloud point temperature, T_{CP}.

In the case of a diblock copolymer consisting of a PNIPAm block and another water-soluble block, the phase transition leads to the formation of micelles with the PNIPAm core and the corona formed by the other block. If the other block is a weak polyelectrolyte, such as poly(methacrylic acid), the copolymer exhibits complex self-assembly behavior dependent on both temperature and pH [6,7].

Amphiphilic copolymers with PNIPAm as a hydrophilic block have markedly different phase transition behavior. Micelles with a hydrophobic core and a PNIPAm corona exhibit the collapse of the dehydrated corona chains above the LCST but the aggregation of the micelles is slower than in the case of PNIPAm homopolymer or does not occur at all [8]. It was proposed that the high density of PNIPAm chains prevents the coronas of colliding micelles from interpenetration and hinders the aggregation [9,10]. The chain density of the PNIPAm corona controlled by the lengths of the PNIPAm blocks affects amphiphilic nonequilibrium thermoresponsive behavior of the micelles resulting in the hysteresis of the cloud point [11]. The kinetics of the growth of aggregates formed by micelles with PNIPAm coronas is affected by structural rearrangement of the aggregates [12–14]. Recently, it was reported that micelles formed by PNIPAm polymers with dodecyl and carboxylic terminal groups (HOOC-PNIPAm-C12) don't undergo phase separation above the LCST of PNIPAm and small angle neutron scattering recognizes the sphere-to-rod transition if carboxylic groups in the peripheral part of the micellar corona are ionized [15].

In this article, we report on the association behavior of HOOC-PNIPAm-C12 polymers in aqueous solutions (Scheme 1) by scattering techniques (light scattering, SAXS) and isothermal titration calorimetry. We show that the synergy of hydrophobic association of PNIPAm induced by the C12 terminal group and of the pH-dependent ionization of the

carboxylate groups affects the thermoresponsive behavior of the polymers and the kinetics of their aggregation above the cloud point temperature T_{CP}.

Experimental section

Materials. *N*-isopropylacrylamide (NIPAM, Aldrich) was recrystallized twice from benzene/n-hexane (1:4 v/v). 4,4′-azobis(isobutyronitrile) (AIBN), from Fluka, was purified by recrystallization from ethanol and subsequently used as a solution in dioxane. 1,4-dioxane (Aldrich) was dried over molecular sieves. S-1-Dodecyl-S$^{'}$-(α,α$^{'}$-dimethyl-α$^{''}$-acetic acid)trithiocarbonate (DTTC), HOOC-terminated PNIPAm (P5) and deuterated chloroform (99 % D) were obtained from Aldrich and used as received.

Table 1 Characteristics of studied PNIPAm polymers

Label	Block composition	$M_w \times 10^{-3}$ (g mol^{-1})[a]	M_w/M_n[a]
C12P6	HOOC-PNIPAm$_{60}$-C$_{12}$H$_{25}$	6.2	1.2
C12P2	HOOC-PNIPAm$_{25}$-C$_{12}$H$_{25}$	2.3	1.2
P5	PNIPAm$_{40}$-COOH	11.1	6.7

[a]Determined by SEC

Scheme 1 Structure of C12P6 and C12P2 polymers

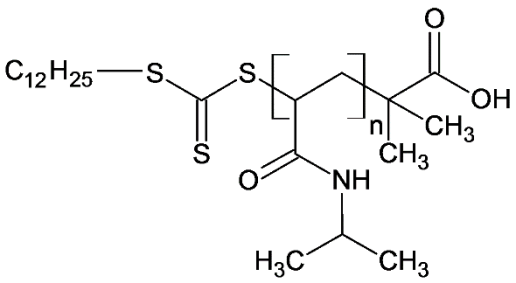

C12P2 and C12P6 synthesis and characterization S-1-Dodecyl-S$^{'}$-(α,α$^{'}$-dimethyl-α$^{''}$-acetic acid)trithiocarbonate (DTTC) solid as the CTA, AIBN as a dioxane solution (moles AIBN : moles CTA = 1:10) and NIPAm monomer were dissolved in dioxane (ca. 5 mL) and placed in a 25 mL round flask with a magnetic stir bar and fitted with a septum. The ampoule was degassed under a stream of N_2 for 20 min and placed in an oil bath at 70 °C, for 6 h. After the end of polymerization, the polymer was precipitated in hexane and dried in a

vacuum oven, at room temperature (yield: 95 %). The CTA utilized incorporates a $C_{12}H_{25}$ hydrophobic group at one end of the PNIPAm polymer and a –COOH at the other.

The sample characterization was performed by ^{1}H NMR spectroscopy and size exclusion chromatography. NMR spectra (See Supporting Information) were recorded at 25°C on a Varian Unity Inova 400 spectrometer. SEC measurements were performed on a Waters system equipped with a Waters 1515 pump, a Waters 2414 differential refractive index detector and Waters HR1, HR4 and HR5E Styragel columns, using THF, containing 3% v/v triethylamine, as the mobile phase at a flow rate of 1.0 mL/min at 40°C. The system was calibrated using a series of monodisperse linear polystyrene standards. Typically, 15 μL of 0.1%w/v solution of the polymers in the carrier solvent was injected in the chromatograph for analysis. The SEC chromatograms are shown in Supporting Information. Molar masses of the used polymers are summarized in Table 1.

Methods Light scattering measurements were carried out with an ALV photometer (ALV, Langen, Germany) consisting of a 22 mW He-Ne laser, operating at the wavelength λ = 632.8 nm, an ALV CGS/8F goniometer, an ALV High QE APD detector and an ALV 5000/EPP multibit, multitau autocorrelator. The cell housing was connected to an external circulation thermostat keeping the constant temperature with the accuracy of ±0.1°C. The temperature dependences were measured at the heating rate of 0.5°C/min. The measurements were carried out at the scattering angle, θ = 90°, corresponding to the scattering vector magnitude, q = 18.7 μm^{-1}.

Dynamic light scattering (DLS) data were evaluated by fitting the electric field autocorrelation function, $g^{(1)}(t,q)$, related to the measured normalized time autocorrelation function of the scattered light intensity, $g^{(2)}(t)$, by the Siegert relation, $g^{(2)}(t)=1+\beta|g^{(1)}(t)|^2$, where β is the coherence factor. The $g^{(1)}(t)$ functions were fitted using the inverse Laplace transform by means of a CONTIN method

$$g^{(1)}(t) = \int_0^\infty A(\tau)\exp\left(-\frac{t}{\tau}\right)\mathrm{d}\tau\,, \qquad (1)$$

Hydrodynamic radius, R_H, can be calculated from τ using the Stokes-Einstein formula, $R_H = k_B T\tau q^2/6\pi\eta$, where k_B is the Boltzmann constant, T is temperature and η is the solvent viscosity.

Small-angle X-ray scattering (SAXS) experiments were carried out on the P12 BioSAXS beamline at the PETRA III storage ring (EMBL/DESY, Hamburg, Germany) at 20°C. The beamline was equipped with a Pilatus 2M detector and synchrotron radiation with

a wavelength of λ = 0.1 nm. The sample-detector distance was 3 m, allowing for covering the q-range interval from 0.07 to 4.4 nm^{-1}. The automatic sample changer for sample volume of 20 μL and cleaning-filling cycle of 1 min was used. The q range was calibrated using the diffraction patterns of silver behenate. The experimental data were normalized to the transmitted beam intensity and corrected for nonhomogeneous detector response, and the background scattering of the solvent was subtracted. The solvent scattering was measured before and after the sample scattering to control for possible sample holder contamination. 20 consecutive frames with 0.05 s exposures comprising the measurement of the solvent, sample, and solvent were performed. Data have been checked for radiation damage. The final scattering curves were processed by automated data acquisition software and recalculated to absolute scattering intensities using the forward scattering of 3.6 mg mL^{-1} bovine serum albumin in 50 mM HEPES pH 7.5 buffer, assuming $(I(0)/c)_{BSA} = 4.84\times10^{-2}$ cm^{-2} mg^{-1} [16]. The data were fitted using the SASfit 0.94.7 software [17].

ζ-Potential measurements were carried out with a Nano-ZS Zetasizer (Malvern Instruments, UK). ζ-Potential values were calculated from electrophoretic mobilities (average of three subsequent measurements, each of which consisted of 15–100 runs) using the Henry equation in the Smoluchowski approximation, $\mu = \varepsilon\zeta/\eta$, where μ is the electrophoretic mobility and ε is the dielectric constant of the solvent.

Isothermal Titration Calorimetry (ITC) measurements were performed with a Nano ITC Isothermal Titration Calorimeter (TA Instruments – Waters LLC, New Castle, DE). The microcalorimeter consists of a reference cell and a 24K gold sample cell. The sample cell is connected to a 50 μL syringe. The syringe needle is equipped with a flattened, twisted paddle at the tip, which ensures continuous mixing of the solutions in the cell rotating at 250 rpm. Titrations were carried out by consecutive 1.01 μL injections of 5 mg mL^{-1} polymer aqueous solutions in water from the syringe into the sample cell filled with 183 μL of water. This method allows for determining the differential heat of mixing for discrete changes of composition. The raw heat changes were analyzed by the NITPIC software [18] in order to obtain ITC thermograms. All experiments were carried out at 25 °C.

pH of solutions was adjusted by titration of aqueous solutions of the polymers (The pH of 1 mg mL^{-1} carboxylated PNIPAm solution was ca. 5) with HCl or NaOH solutions so that the total concentration of HCl ranged from 10^{-4} to 10^{-2} M and of NaOH from 10^{-5} to 10^{-2} M. The pH measurements were carried out with a Thermo Scientific Orion Star A211 pH meter equipped with a 8302B glass electrode.

Results and discussion

C12Px self-assembly in aqueous solution Scattering measurements confirm that C12Px polymers undergo micellization in aqueous media as reported previously [15]. The SAXS curves of C12P6 and C12P2 in weakly basic (pH 8) aqueous solutions curves are shown in Fig. 1. The CONTIN distributions of hydrodynamic radii of the polymers in the insert of Fig. 1 are bimodal, revealing that all three polymer solutions contain fractions of large aggregates. The aggregation manifests itself also in the SAXS behavior in the low q region (q < 0.1 nm^{-1}) so that the scattering intensities do not reach the Rayleigh regime and rise with decreasing q following the power law, which indicates the presence of aggregates.

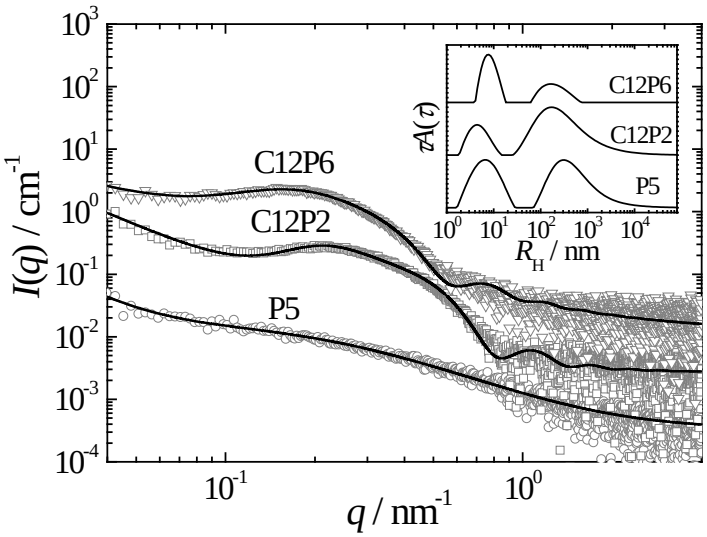

Fig. 1 SAXS curves for 10 mg mL^{-1} for P5, C12P2 and C12P6 solutions at pH 8. The curves are separated by the multiplicative factor of 5 for clarity. Insert shows CONTIN distributions of hydrodynamic radii for 1 mg mL^{-1} P5, C12P2 and C12P6 solutions at pH 8.

In the case of the P5 polymer, the Guinier regime in mid-q region is followed by a power law behavior with the exponent α = ~–1.5 which indicates that P5 dissolves as individual polymer coils. In contrast to the P5 polymer, C12-terminated PNIPAms exhibit much more pronounced Guinier regimes in the mid q-range followed by the Porod limit scattering behavior ($I(0) \sim q^{-4}$) which accords with the assumption that these polymers form compact spherical micelles with the core of the C12 terminal groups and the corona of the PNIPAm chains. The Guinier regime of both C12P2 and C12P6 is preceded by a shallow minimum in the scattering intensity caused by the interparticle correlation due to electrostatic repulsion between carboxylate groups located on the periphery of the micellar corona.

Taking these considerations into account, the P5 scattering, $I_{P5}(q)$, was treated by the form factor of polydisperse Gaussian coils, with the fixed value of the dispersity index, $d = M_w/M_n = 6.7$, obtained from SEC, while the micellar scattering, $I_{C12Px}(q)$, was fitted by a simplified model of homogeneous spheres interacting with the screened electrostatic potential. The P5 scattering is thus described by the equation

$$I_{P5}(q) = N_c(\Delta b_c)^2 P_{gc}(q; R_g, d) + I_1 q^{-\alpha} + I_0 \quad (2)$$

where I_1, I_0, α are the parameters describing the background and the power-law scattering from the aggregates, N_c is the number of polymer coils in the unit volume, b_c is the excess scattering lengths of the coils and $P_{GC}(q, R_g, d)$ is the form factor of polydisperse Gaussian coils with the dispersity index d and the mean radius of gyration R_g.

The C12Px scattering is fitted to the equation

$$I_{C12Px}(q) = N_m(\Delta b_m)^2 S_{HP}(q; R_{int}, z, \varepsilon, T, s, \varphi) P_{sph}(q, R) + I_{1m} q^{\alpha_m} + I_{0m} \quad (3)$$

where I_1, I_0 and α have the same meaning as in eq. 2, N_m and Δb_m, respectively, are the number density and the scattering length of the micelles, $P_{sph}(q,R) = [3\sin(qR)-qR\cos(qR)]^2/(qR)^6$ is the form factor for the homogeneous sphere with the radius R and $S_{HP}(q,R_{int},z,\varepsilon,T,s,\varphi)$ is the Hayter-Penfold structure factor for hard spheres with screened repulsive electrostatic interaction [19]. Here R_{int} is the interaction radius of the sphere, set to be equal to the sphere radius in the form factor, z is the charge number of the sphere, set to be equal to the aggregation number of the micelles (see below), $\varepsilon = 81$ is the relative dielectric permittivity of water, $T = 293$ K is the temperature, $s = 40$ μM is the monovalent salt concentration (corresponding to the concentration of NaOH used to adjust to pH of the solution to 8) taken for the calculation of the Debye screening length and φ is the volume fraction of the spheres.

Table 2 Parameters of studied PNIPAms obtained by SAXS and DLS

polymer	R, nm	R_g, nm	R_H, nm	N_{agg}, nm	α
P5	–	7.3	5.9	–	1.90
C12P2	5.4	–	5.4	19.4	2.05
C12P6	7.7	–	7.8	13.8	1.39

The simplification applied for the treatment of the micellar scattering can be justified by the fact that the core volume is much smaller than that of the corona, so that the scattering behavior of the micelles is close enough to that of a homogeneous sphere. Since the mass concentrations and scattering length densities of the polymers are equal, the molar mass of the micelles can be estimated from forward scattering intensities as

$$M_{\mathrm{w,\,C12Px}} = \frac{I_{\mathrm{C12Px}}(0)}{I_{\mathrm{P5}}(0)} M_{\mathrm{w,P5}} \qquad (3)$$

The results of the SAXS data evaluation are summarized in Table 2 and fits shown in Fig. 1. The sphere radii obtained from SAXS are in good accordance both with the hydrodynamic radii obtained by DLS and with the previously reported micellar radii of C12-terminated PNIPAms of comparable molar masses obtained by SANS [15].

We carried out ITC measurements in order to follow thermal processes connected with association of C12-termimated PNIPAms. ITC measurements (Fig. 2) revealed that the dilution of C12P2 and C12P6 in water is an exothermic process with the corresponding enthalpy about –5 kJ mol^{-1} for both polymers. The observed exotherm reflects the demicellization of C12-terminated PNIPAms and subsequent hydration of the dodecyl groups.

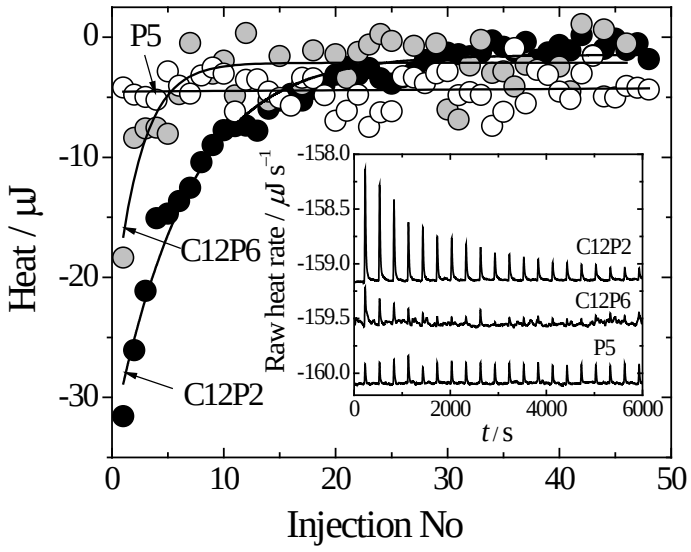

Fig. 2 Enthalpy curves for titrating 5 mg mL^{-1} P5, C12P2 and C12P6 solution into water. Insert shows the raw ITC data.

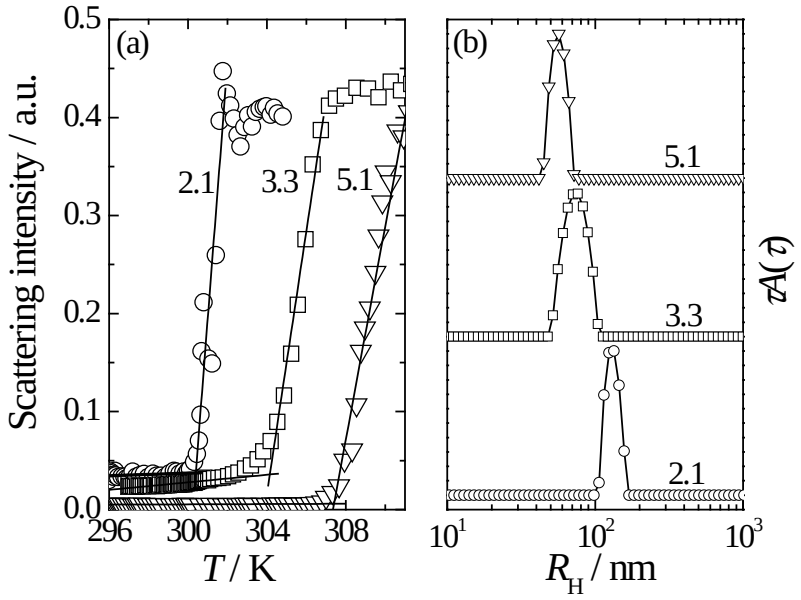

Fig. 3 (a) Scattering intensities at $\theta = 90°$ for 1 mg mL^{-1} C12P6 aqueous solutions at various pH (indicated at the individual curves) as functions of temperature. (b) CONTIN distributions of hydrodynamic radii for C12P6 aqueous solutions at various pH (indicated at the individual curves) measured at T_{cp}

C12Px thermoresponsive and pH-responsive behavior Light scattering measurements reveal that the cloud point temperatures, T_{CP}, of C12-terminated PNIPAms, as well as the hydrodynamic radii, R_H, of C12-terminated PNIPAm aggregates formed after reaching T_{CP}, are pH-dependent (Fig. 3), unlike the T_{CP} and R_H of P5. Fig. 4 shows the T_{cp} and ζ potential as functions of pH for all three studied PNIPAms. The ζ potential becomes negative in the alkaline region due to the ionization of the terminal COOH group. While for C12P2 and C12P6, the ζ potential dependences correlate with those of T_{CP}, the T_{CP} of P5 is pH-independent (Fig. 4a) unlike its ζ potential. This fact indicates that the ionization state of the terminal carboxylate group affects the hydration of the PNIPAm chain in the micellar corona but not that of the free PNIPAm chain. Moreover, the pH dependence of hydrodynamic radii of the aggregates in the case of C12-terminated PNIPAms suggests that the phase separation in affected also by kinetic effects and the rate of aggregation is influenced by the electrostatic repulsion between charged micellar coronas.

In order to assess the influence of electrostatic screening on the thermoresponsive behavior, we studied temperature dependences of light scattering from the PNIPAm solution at various ionic strengths. The ionic strength was adjusted by sodium iodide, which is known

to have almost no influence (unlike many other salts) on the LCST behavior of PNIPAm due to hydration effects [20].

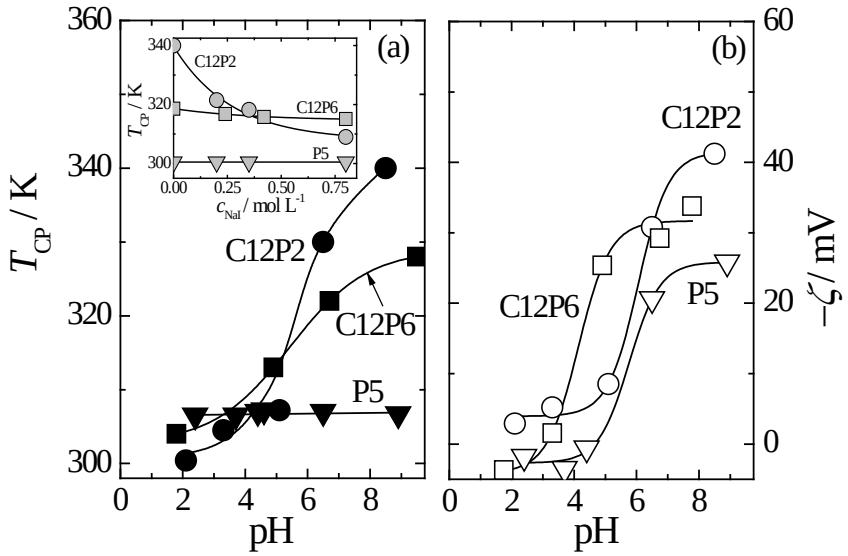

Fig. 4 (a) Cloud point temperatures of 1 mg ml^{-1} P5, C12P2 and C12P6 aqueous solutions as functions of pH. Insert shows the T_{CP} of P5, C12P2 and C12P6 solutions at pH 5.8 as functions of sodium iodide concentration. (b) The negative ζ potentials, $-\zeta$, of 1 mg ml^{-1} P5, C12P2 and C12P6 aqueous solutions as functions of pH

Surprisingly, while C12P2 exhibits a strong decrease in the T_{CP} in alkaline solutions with the increasing NaI concentration, the T_{CP} of C12P6 remains almost unaffected (Fig. 4a Insert) which suggests that the observed shifts in T_{CP} are connected rather with the changes of the solvation of the micellar corona. Since C12P6 micelles are larger and have a lower association number than C12P2 micelles, the resulting lower density of PNIPAm segments in the corona makes them less sensitive to changes in hydration induced by the ionization of the terminal carboxylic groups, which explains why the observed shifts in T_{CP} for C12P6 are lower than for C12P2 and are less affected by ionic strength.

On the other hand, both C12P2 and C12P6 exhibit a strong increase in the rate of the growth of the size of the aggregates after reaching T_{cp}. The time dependences of R_H of C12Px aggregates in alkaline solutions (pH 8) at temperatures exceeding T_{cp} (T = 328 K) and various ionic strengths are shown in Fig. 5. Insert in Fig. 5b shows the hydrodynamic radii of the aggregates after 5000 s at 328 K as functions of the NaI concentration, indicating that the aggregation is accelerated at high ionic strength. The fastest step of the phase separation process is the formation of aggregates which occur on the timescales comparable with the time required for thermal equilibration of the sample ($t < 10^2$ s). At the later stage of the

process, the radius of the aggregates grows with time as $R_H(t) \sim \log t$ which is typical for systems in which the activation energy of coagulation is proportional to the size of the aggregates and in which the aggregates easily rearrange so that they adopt compact spherical structures [21]. The latter condition is fulfilled due to the high fluidity of the small core of C12Px micelles. A similar behavior was reported for the aggregation of soft PS–PNIPAm–PS block copolymer micelles in water–methanol mixtures [12].

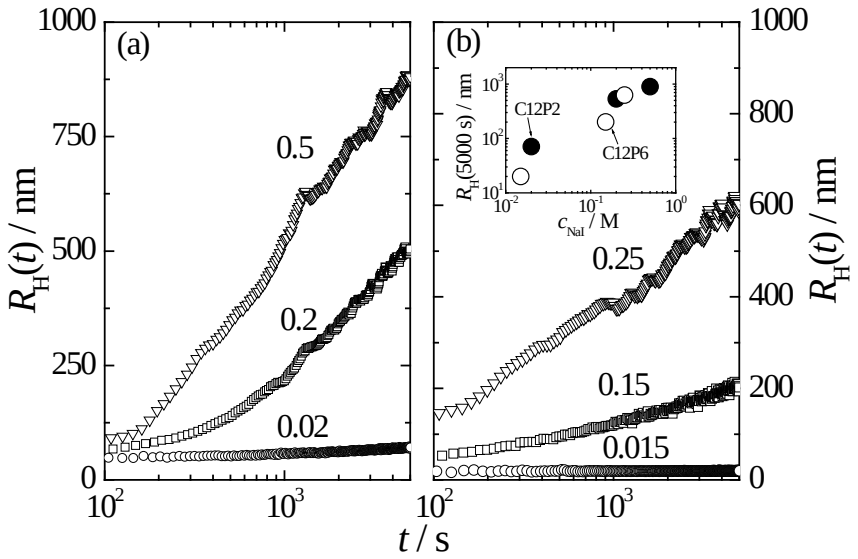

Fig. 5 $R_H(t)$ vs. t for (a) C12P2 and (b) C12P6 solutions at various NaI concentration (given at individual curves in mol L^{-1}) and pH 8 after heating at 328 K. Insert: R_H of C12P2 and C12P6 aggregates at 5000 s after incubation at 328 K vs. sodium iodide concentration

Conclusions

We have studied the association behavior of two PNIPAm polymers, C12P2 and C12P6, each with dodecyl and carboxylate terminal groups (Scheme 2), in aqueous solutions as a function of temperature, pH and ionic strength. As the hydration state of PNIPAm chains in the micelles is affected by ionization/protonation of the carboxylate group, changing pH of the solution allows for tuning the temperature of the phase separation of the system (detected by light scattering as the cloud point temperature, T_{CP}). The effect of pH on T_{CP} is more pronounced for C12P2 due to the higher association number and smaller size of C12P2 micelles, which result in a denser micellar corona compared to C12P6. The rate of aggregation of both C12P2 and C12P6 in alkaline solutions above T_{CP} can be decreased by

increasing the ionic strength of the solution which proves that the aggregation kinetics of these polymers can be controlled by screening the electrostatic repulsion between the carboxylate end groups in the micellar coronas.

Scheme 2 Phase separation of C12Px polymers

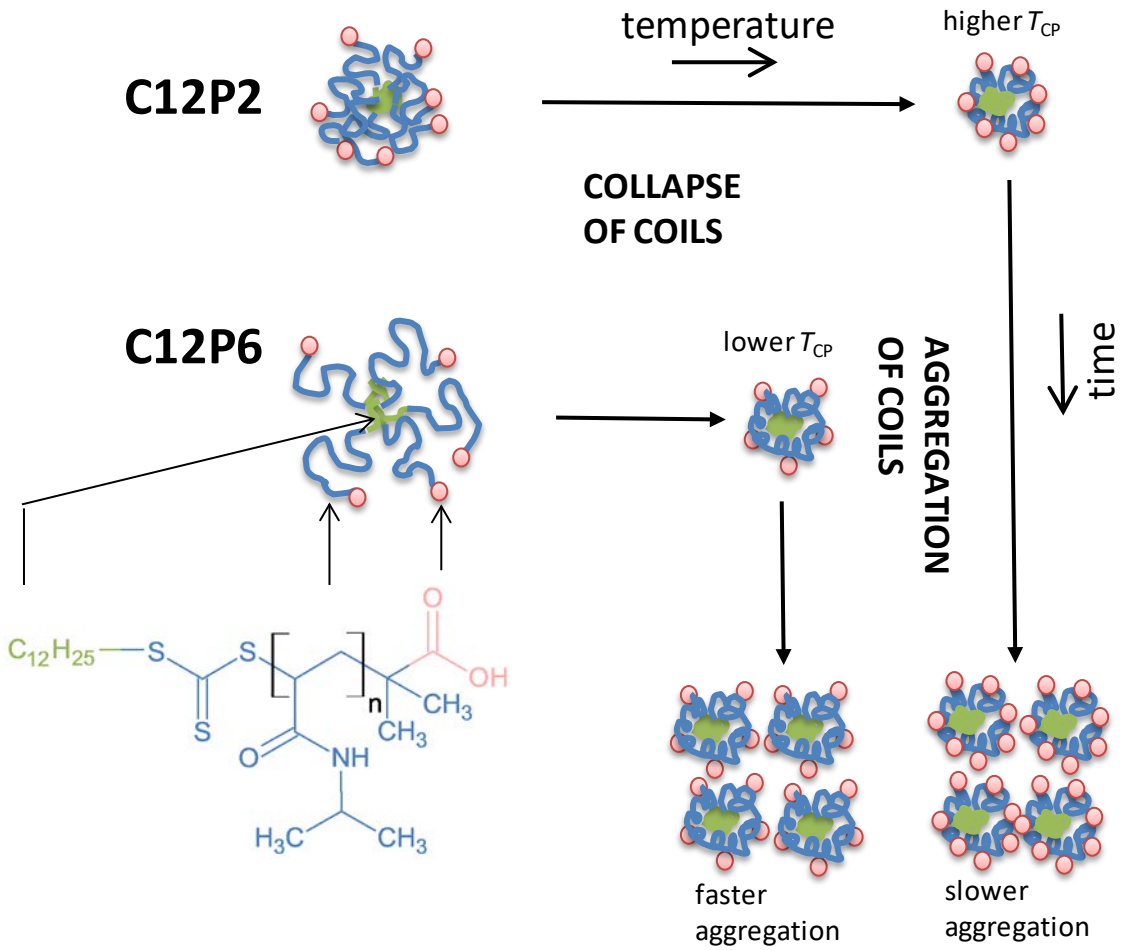

Acknowledgments

M. Š. acknowledges the support from the Czech Science Foundation (Grant No. 14-11516S). The support of Clement Blanchet (EMBL) is kindly acknowledged.

References

1. Dai ZJ, Ngai T (2013) Microgel particles: The structure-property relationships and their biomedical applications. J Polym Sci A Polym Chem 51:2995–3003. DOI: 0.1002/pola.26698

2. Hu L, Sarker AK, Islam MR, Li X, Lu ZZ, Serpe MJ (2013) Poly(N-isopropylacrylamide) microgel-based assemblies. J Polym Sci A Polym Chem 51:3004–3020. DOI: 10.1002/pola.26702
3. Hocine S, Li MH (2013) Thermoresponsive self-assembled polymer colloids in water. Soft Matter 9:5839–5861. DOI: 10.1039/c3sm50428j
4. Chan K, Pelton R, Zhang J (1999) On the formation of colloidally dispersed phase-separated poly(N-isopropylacrylamide). Langmuir 15:4018–4020. DOI: 10.1021/la9812673
5. Cao ZQ, Liu WG., Gao P, Yao KD, Li HX, Wang GC (2005) Toward an understanding of thermoresponsive transition behavior of hydrophobically modified N-isopropylacrylamide copolymer solution. Polymer 46:5268–5277. DOI: 10.1016/j.polymer.2005.04.050
6. Li GY, Song S, Guo L, Ma SM (2008) Self-assembly of thermo- and pH-Responsive poly(acrylic acid)-b-poly(N-isopropylacrylamide) micelles for drug delivery. J Polym Sci A Polym Chem 46:5028–5035. DOI: 10.1002/pola.22831
7. Schilli CM, Zhang MF, Rizzardo E, Thang SH, Chong YK, Edwards K, Karlsson G, Müller AHE (2004) A new double-responsive block copolymer synthesized via RAFT polymerization: Poly(N-isopropylacrylamide)-block-poly(acrylic acid). Macromolecules 21:7861–7866. DOI: 10.1021/ma035838w
8. Nuopponen M, Ojala J, Tenhu H (2004) Aggregation behaviour of well defined amphiphilic diblock copolymers with poly (N-isopropylacrylamide) and hydrophobic blocks. Polymer 45:3643–3650. DOI: 10.1016/j.polymer.2004.03.083
9. Zhang WA, Zhou XC, Li H, Fang Y, Zhang GZ (2005) Conformational transition of tethered poly(N-isopropylacrylamide) chains in coronas of micelles and vesicles. Macromolecules 38:909–914. DOI: 10.1021/ma048227s
10. Ye XD, Fei JY, Guan J, Zhou XC, Zhang GZ (2010) Dispersion of Polystyrene Inside Polystyrene-b-poly(N-isopropylacrylamide) Micelles in Water. J Polym Sci B Polym Phys 48: 749–755. DOI: 10.1002/polb.21948
11. Blackman LD, Wright DB, Robin MP, Gibson MI, O'Reilly RK (2015) Effect of Micellization on the Thermoresponsive Behavior of Polymeric Assemblies. ACS Macro Lett. 4:1210–1214. DOI: 10.1021/acsmacrolett.5b00551
12. Kyriakos K, Philipp M, Adelsberger J, Jaksch S, Berezkin AV, Lugo DM, Richtering W, Grillo I, Miasnikova A, Laschewsky A, P Müller-Buschbaum P, Papadakis CM (2014) Cononsolvency of Water/Methanol Mixtures for PNIPAM and PS-b-PNIPAM:

Pathway of Aggregate Formation Investigated Using Time-Resolved SANS. Macromolecules 47:6867–6879.

13. Adelsberger J, Kulkarni A, Jain A, Wang WN, Bivigou-Koumba AM, Busch P, Pipich V, Holderer O, Hellweg T, Laschewsky A, Müller-Buschbaum P, Papadakis CM (2010) Thermoresponsive PS-b-PNIPAM-b-PS Micelles: Aggregation Behavior, Segmental Dynamics, and Thermal Response. Macromolecules 43:2490–2501. DOI: 10.1021/ma902714p
14. Papagiannopoulos A, Zhao JP, Zhang GZ, Pispas S, Radulescu A (2014) Thermoresponsive aggregation of PS-PNIPAM-PS triblock copolymer: A combined study of light scattering and small angle neutron scattering. Eur Polym J 56:59–68. DOI: 10.1016/j.eurpolymj.2014.04.013
15. FitzGerald PA, Gupta S, Wood K, Perrier S, Warr GG (2014) Temperature- and pH-Responsive Micelles with Collapsible Poly(N-isopropylacrylamide) Headgroups (2014) Langmuir 30:7986–7992. DOI: 10.1021/la501861t
16. Mylonas E, Svergun DI (2007) Accuracy of molecular mass determination of proteins in solution by small-angle X-ray scattering. J Appl Cryst 40:S245–S249. DOI: 10.1107/S002188980700252X
17. Bressler I, Kohlbrecher J, Thünemann AF (2015) SASfit: a tool for small-angle scattering data analysis using a library of analytical expressions. J Appl Cryst 48:1587–1598.
18. Keller S, Vargas C, Zhao HY, Piszczek G, Brautigam CA, Schuck P (2012) High-Precision Isothermal Titration Calorimetry with Automated Peak-Shape Analysis. Anal Chem 84:5066–5073. DOI: 10.1021/ac3007522
19. Hayter JB, Penfold J (1981) An analytic structure factor for macroion solutions. Mol Phys 42:109–118. DOI: 10.1080/00268978100100091
20. Zhang YJ, Furyk S, Bergbreiter DE, Cremer PS (2005) Specific ion effects on the water solubility of macromolecules: PNIPAM and the Hofmeister series. J Am Chem Soc 127:14505–14510. DOI: 10.1021/ja0546424
21. Brey JJ, Prados A (2001) Slow logarithmic relaxation in models with hierarchically constrained dynamics. Phys Rev E 63:021108. DOI: 10.1103/PhysRevE.63.021108